High-performance Hg^{2+} removal from ultra-low-concentration aqueous solution using both acylamide- and hydroxyl-functionalized metal-organic framework

Feng Luo,* Jing Li Cheng, Li Long Dang, Wei Na Zhou, Hai Lv Lin, Jiang Qiang Li, Shu Juan Liu, and Ming Biao Luo

Table S1 Adsorption isotherm constants for Hg^{2+} onto MOF material.

Langmuir isotherm			Freundlich isotherm		
q_{max}	K_L	R^2	K_F	$1/n$	R^2
mg g^{-1}	mg L^{-1}		mg g^{-1}		
333.33	2.776	0.9145	71.593	0.671	0.816

Table S2 Thermodynamic parameters for sorption of Hg^{2+}.

ΔH^0(kJ mol^{-1} k^{-1})	ΔS^0(J mol^{-1} k^{-1})	ΔG^0 (kJ mol^{-1})		
		298.15	308.15	318.15
-3.93	67.33	-24.01	-24.68	-25.35

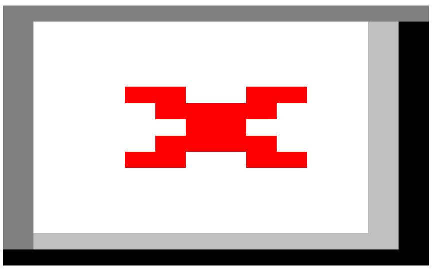

Fig. S1 PXRD patterns simulated from single crystal data, of synthesized samples and Hg^{2+} loaded samples.

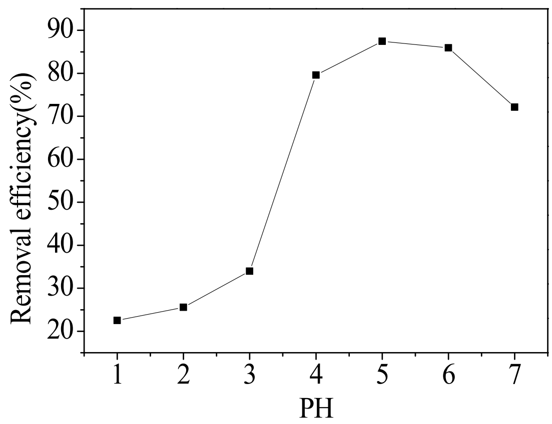

Fig. S2 pH effect on the adsorption of Hg^{2+} ($c_0(Hg^{2+})$=100 ppb, v=40 mL, m(adsorbent)=2 mg, T=25℃, t=2 h).

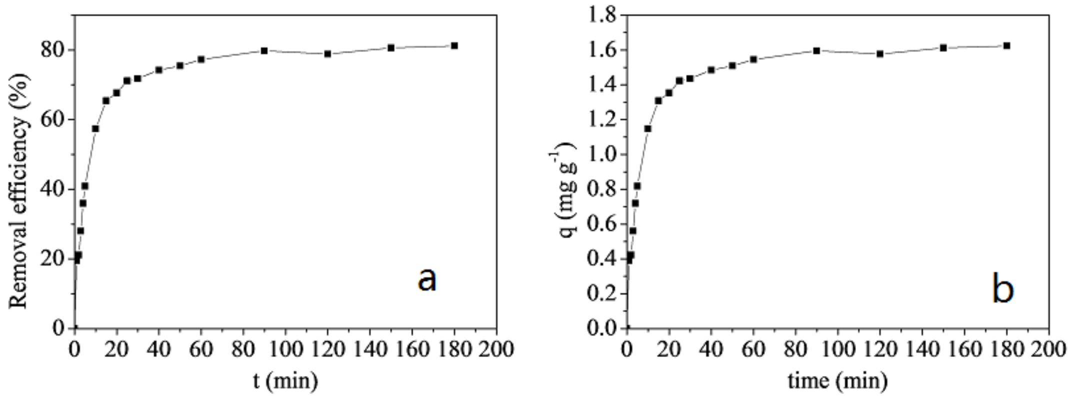

Fig. S3 Effect of contact time on Hg(Ⅱ) removal ($c_0(Hg^{2+})$=100 ppb, v=40 mL, m(adsorbent)=2 mg, T=25℃, pH=5)

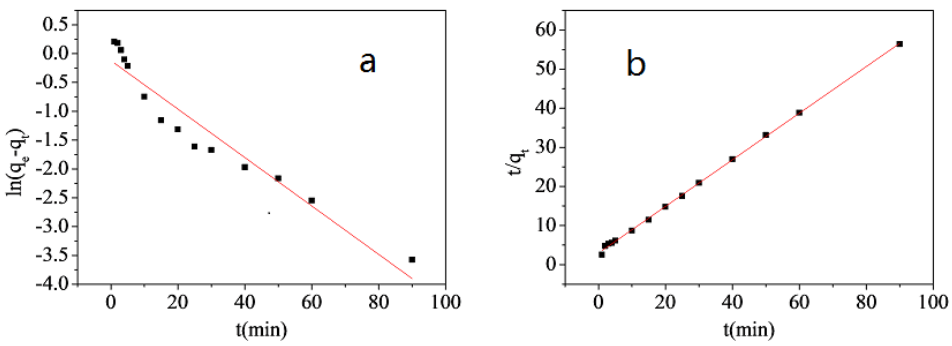

Fig. S4 Pseudo-first-order kinetic plot (a) and pseudo-second-order kinetic plot (b) for the adsorption of Hg(II) onto adsorbent.

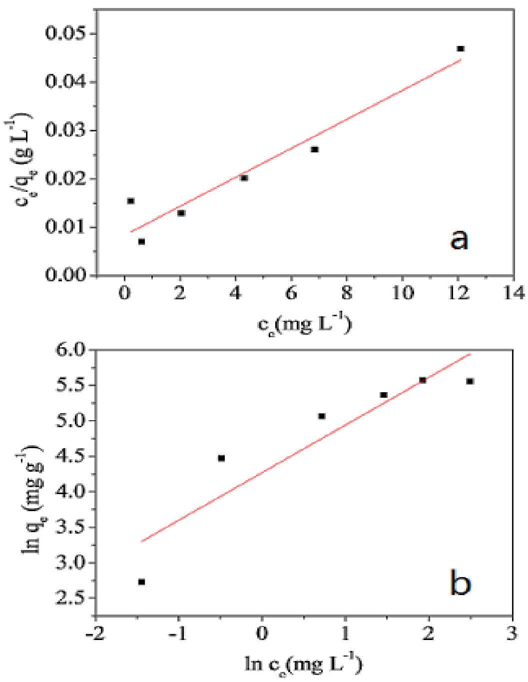

Fig. S5 Adsorption isotherms fitted by the Langmuir (a) and Freundlich (b) models (c_0(Hg^{2+})=100 ppb, v=40 mL, m(adsorbent)=2 mg, T=25℃, t=1 h).

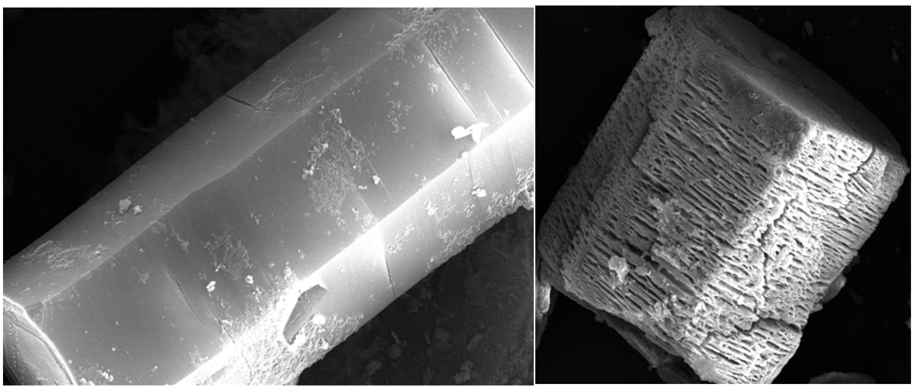

Fig. S6 The TEM image of the MOF material before and after the adsorption of Hg(II).

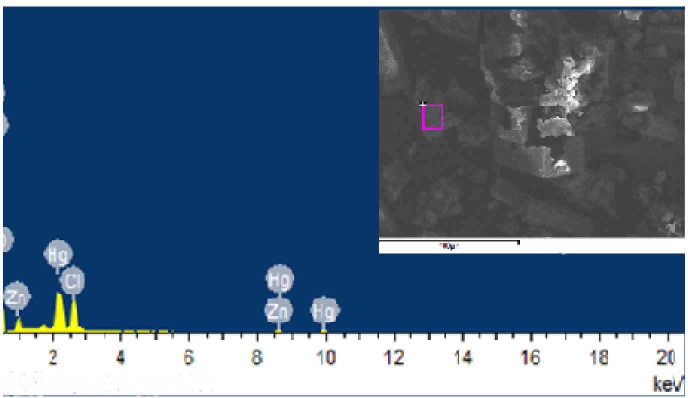

Fig. S7 SEM and EXD spectra of the MOF material after loading Hg^{2+}.

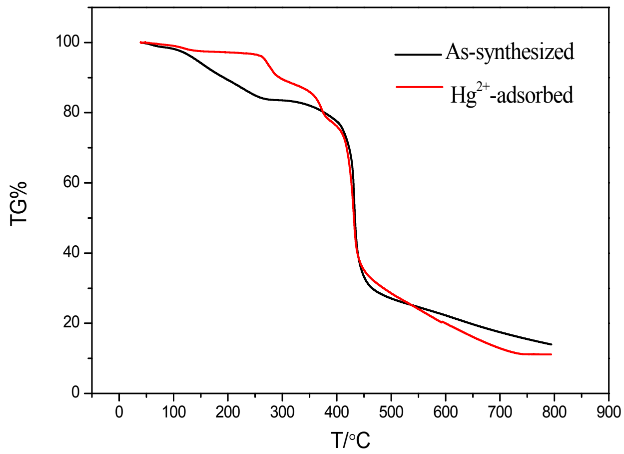

Fig. S8 TG curves of as-synthesized and Hg^{2+}-adsorbed MOF sample.